CONFIDENTIAL

# *Calibration Report on the University of Michigan Supersonic Wind Tunnel*

## *Part I -Wind Tunnel Facilities and Testing Techniques*

## *Part II -Aerodynamic Calibration at Nominal Mach Number of 1.90*


*by*

*P. E. Culbertson*

*Approved by*

*L. C. Garby*
*Engineer-in-Charge*

*H. P. Liepman*
*Director*
*Supersonic Wind Tunnel*



*Project MX-794*

*(USAF Contract No. W33-038-ac-14222)*





*November 1949*


CONFIDENTIAL

## ACKNOWLEDGEMENTS

The author wishes to make grateful acknowledgement to those members of the Wind Tunnel Staff who assisted in obtaining the data presented in this report; and to the members of the Wind Tunnel Committee whose technical advice and editorial comments made the report possible.

TABLE OF CONTENTS

| | Page |
|---|---|
| List of Figures | ii |
| Nomenclature | iii |
| Part I - Wind Tunnel Facilities and Testing Techniques | |
| Summary | 1 |
| A. Introduction | 2 |
| B. Measuring Facilities | 4 |
| C. Calibration | 5 |
| 1. Pressure Measurement, Mach Number Determination and Experimental Accuracies | 6 |
| 2. Model Size Criteria | 13 |
| 3. Flow Inclination | 14 |
| 4. Length of Run | 16 |
| 5. Influence of Dew Point | 17 |
| Part II - Aerodynamic Calibration at Nominal Mach Number of 1.90 | |
| Summary | 18 |
| 1. Pressure and Mach Number Distribution | 20 |
| 2. Blocking | 27 |
| 3. Flow Inclination | 29 |
| 4. Length of Run | 31 |
| 5. Influence of Dew Point | 33 |
| Appendix | |
| A. Accuracy of the Determination of Static Pressure From Stagnation and Total Head Pressures | 34 |
| B. Standard deviation of Pressure Coefficient Due to Error in Pressure Measurement. | 35 |
| C. Pressure Correction Evaluation | 36 |
| References | 39 |

## LIST OF FIGURES


| | | Page |
|---|---|---|
| I-1 | Wind Tunnel Components | 3 |
| 2 | Test Section Cutaway Showing Fixed Strut Locations | 5 |
| 3 | Test Section Cutaway Showing Arc Sector Strut | 5 |
| 4 | Photograph of 5 Prong Static Probe | 11 |
| 5 | Photograph of 5 Prong Total Head Probe | 12 |
| 6 | Photograph of Flow Inclinometer | 15 |
| II-1 | Mach 1.90 Nozzle Coordinates | 19 |
| 2 | Test Section Static Pressure Gradient at Mach 1.90 | 21 |
| 3 | Test Section Static Pressure Gradient at Mach 1.90 | 22 |
| 4 | Test Section Centerline Mach Number, Dynamic Pressure and Static Pressure Gradients | 23 |
| 5 | Test Section Wall pressures and a Summary of Visible Shock Waves at Mach 1.90 | 24 |
| 6 | Schlieren of Model-Free Flow at Mach 1.90 | 25 |
| 7 | Nozzle Wall Pressure Distribution at Mach 1.90 | 26 |
| 8 | Summary of Blocking Characteristics at Mach 1.90 | 28 |
| 9 | Flow Inclination with Respect to the Horizontal Plane at Mach 1.90 | 30 |
| 10 | Flow Inclination with Respect to the Vertical Plane at Mach 1.90 | 30 |
| 11 | Run Time at Mach 1.90 | 31 |
| 12 | Run Time at Mach 1.90 | 32 |
| 13 | Static Sidewall Pressure as a Function of Dew Point at Mach 1.90 | 33 |
| 14 | Uncorrected Pressure Coefficient Over a $15^{\circ}$ Cone at Mach 1.90 | 37 |
| 15 | Corrected Pressure Coefficient Over a $15^{\circ}$ Cone at Mach 1.90 | 38 |

## NOMENCLATURE

$M$ = Local Mach Number

$P_s$ = Static Pressure

$P_o$ = Stagnation Pressure

$P_a$ = Ambient Static Pressure

$P_o'$ = Stagnation Pressure Immediately Downstream of a Normal Shock Wave

$P^o$ = Stagnation Pressure in the Vacuum Tank Before a Run

$P_f$ = Stagnation Pressure in the Vacuum Tank at the End of a Run

$P_b$ = Atmospheric Pressure

$t$ = Length of Run

$v$ = Vacuum Tank Volume

$C_p$ = Pressure Coefficient = $\frac{2}{\gamma}\left(\frac{P_s - P_a}{P_a M^2}\right)$

$\gamma$ = Ratio of Specific Heats = 1.4

$A$ = Test Section Area

$a_o$ = Stagnation Speed of Sound

$\sigma$ Indicates Standard Deviation

Part I

# WIND TUNNEL FACILITIES

# AND TESTING TECHNIQUES

## SUMMARY

Part I of this report contains a description of general tunnel characteristics and measuring facilities available without regard to a specific Mach number. The subsequent sections present the aerodynamic flow calibration of the tunnel at specific Mach numbers. At present this will include only the Mach 1.90 configuration. As additional nozzle blocks are calibrated, supplementary sections will be added to this basic report.

A description and analysis of the force measuring facilities available will be the subject of a separate report.

## A. INTRODUCTION

The University of Michigan supersonic wind tunnel is an intermittent vacuum type, with its operating potential resulting from the pressure differential between air stored at atmospheric pressure and the low pressure of an evacuated tank. The tunnel utilizes a closed circuit which decreases the magnitude of the problem of cleaning and drying the air to the conditions necessary for the range of tests performed. A diagrammatic sketch of the tunnel components, showing their relative location, is presented in Figure I-1.

This figure shows the 24,000 cubic foot fabric storage bag, its outlet to the tunnel channel, the turbulence screens, the removable nozzle blocks, the test section and balance system housing, the diffuser, the master valve, and outlet into the 13,000 cubic foot vacuum tanks. The air is drawn from the vacuum tanks by the vacuum pump, forced through the surge tank, through the precipitron filters, and into the storage bag. A separate circuit continuously draws air from one end of the storage bag, through a dryer utilizing activated alumina, and back into the bag.

The tunnel channel consists of the nozzle region, the test section, and the diffuser. The test Mach number is obtained by the use of removable nozzle blocks. These blocks are 56" in length and span the 8" width of the tunnel. They are readily insertable, making the change from one Mach number to another a simple matter. The test section of the tunnel is of uniform cross-section, uncorrected for boundary layer, 8" wide and 13" deep with an overall length of 45". The test section sidewalls are fitted with optically ground windows, 16" in diameter, for Schlieren photograph and visual observation. The various provisions for the mounting of models within the test section are described in Part I-C of this report.

An external balance system is housed in a box which surrounds the test section. Forces on a model are transmitted by a force strut from the test section through the top and bottom tunnel walls to the balance system (Ref. 1). A second balance system, integral with the model sting, is currently being developed (Ref. 2). The balance systems are the subject of a separate report.

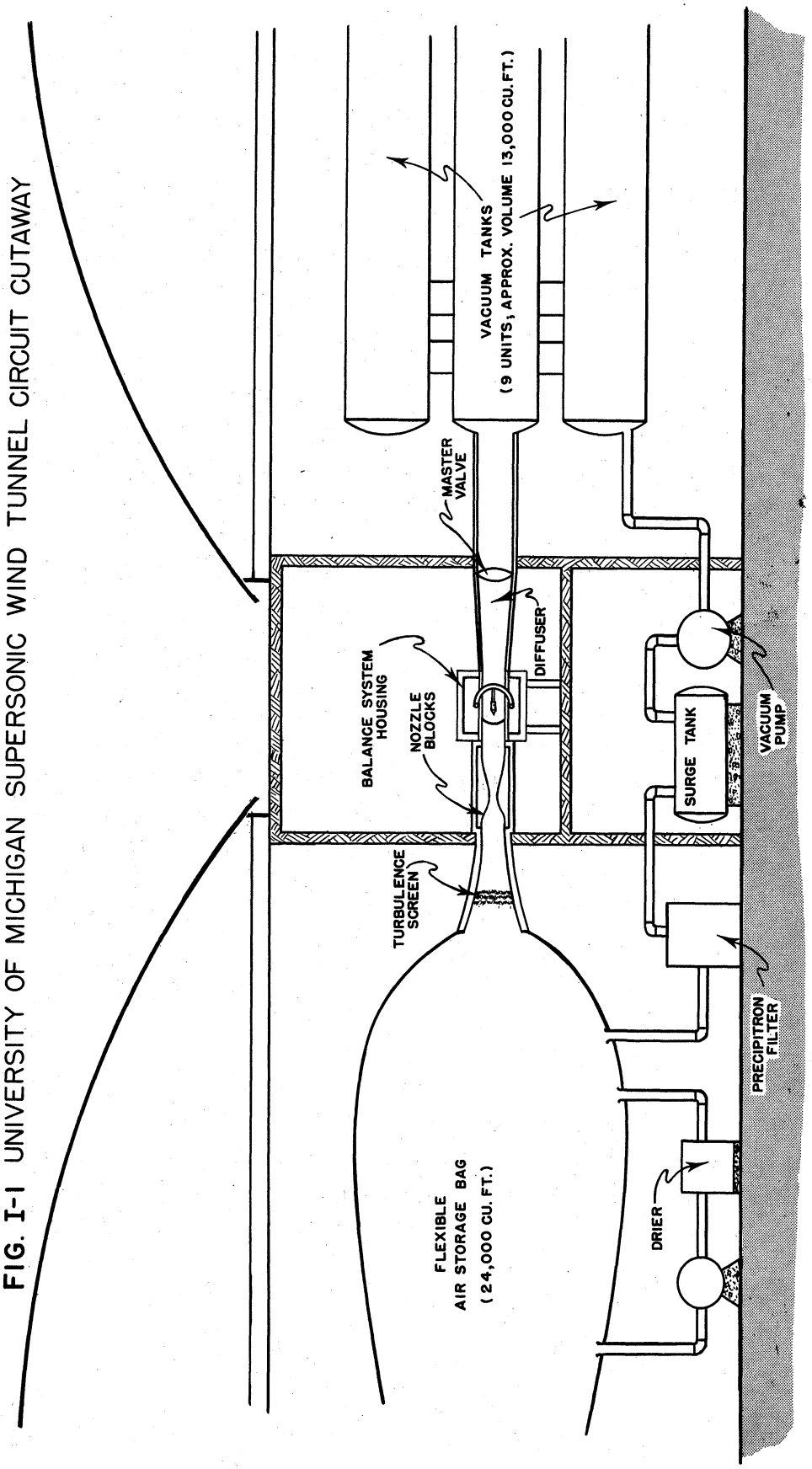


FIG. I-1 UNIVERSITY OF MICHIGAN SUPERSONIC WIND TUNNEL CIRCUIT CUTAWAY

## B. MEASURING FACILITIES

The facility is equipped to make pressure measurements at as many as 100 locations for each run; to measure lift up to 100 pounds, pitching moment up to 2640 inch pounds, and drag up to 200 pounds; and to take Schlieren and shadowgraph photographs.

Pressures are determined by manometer board measurements. The manometer board currently in use consists of four separate banks of 25 tubes each. Each bank is connected, through a manifold, to a reservoir, having as its reference any pressure desired. Thus it is possible to use simultaneously four different fluids and/or reference pressures if the nature of the tests makes such a configuration desirable. A photograph of the manometer board is taken on 4" x 5" film during the run, at a time when the manometer fluid has reached its equilibrium condition. Pressure data are then read from suitable photographic prints.

The wind tunnel optical equipment consists of a single coincidence Schlieren system, being suitable for conversion to shadowgraph. The system utilizes a high intensity mercury vapor slit type light source, reflection by two 18 inch parabolic mirrors of 10 feet focal length, cutoff knife edge, and camera. It is possible to orient the source slit and knife edge either horizontally or vertically to facilitate flow studies. Minimum camera exposure time is 4 microseconds. It is also possible to take Schlieren movies of the test section at speeds up to 5,000 frames per second.

## C. CALIBRATION

The aerodynamic calibration of the wind tunnel at specific Mach numbers consists of a study of the flow pressures and inclinations within the test section, the physical limitations on model configurations which can be tested in the tunnel, a determination of the length of run possible for given initial pressure differentials, a study of various other physical limitations in testing, and a discussion of the accuracies obtainable with the instrumentation available.

The actual flow probing is possible, through the use of a variety of strut configurations and locations as indicated in Figures 2 and 3, from a position 20" upstream to 8" downstream of the test section centerline. Of this, the most significant region is that from 8" upstream to 8" downstream of the centerline, inasmuch as that is the visually observable area as well as the region in which the vast majority of models are located. Sufficient calibration data are obtained for a quantitative evaluation of the data obtained during actual testing.

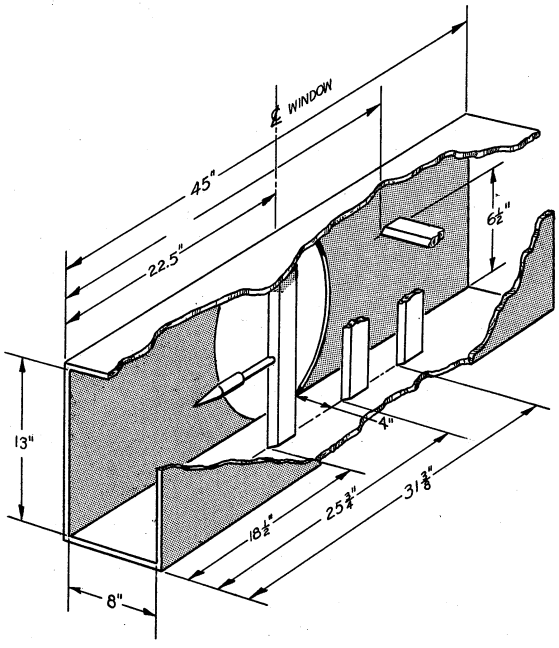


FIGURE I-2

TEST SECTION CUTAWAY SHOWING FIXED STRUT LOCATIONS

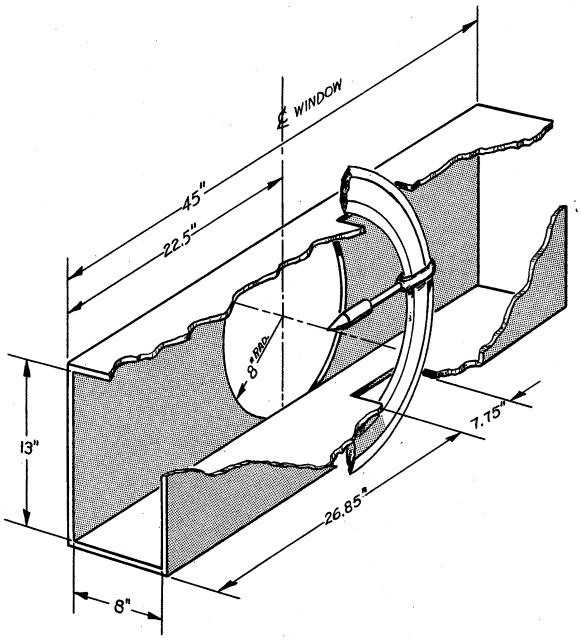


FIGURE I-3

TEST SECTION CUTAWAY SHOWING ARC SECTOR STRUT

## 1. PRESSURE MEASUREMENT, MACH NUMBER DETERMINATION, AND EXPERIMENTAL ACCURACIES

Because the flow in the test section is usually not uniform, a rather complete determination of local ambient pressure, Mach number, and flow inclination is necessary in order to interpret the data obtained during testing.

Non-uniformities are produced by many factors. The fact that the test section is uniform in cross-section introduces a gradual increase in static pressure with a resulting decrease in Mach number due to boundary layer build-up. The extent to which the nozzle blocks differ, either in design or in fabrication, from a theoretically correct contour introduces local variations. Imperfections in the tunnel surface and in the juncture between the nozzle blocks and the test section create local disturbances. Although these latter factors are held within rigid specifications, minute discrepancies produce irregularities in the flow which contribute to the necessity for a complete determination of flow conditions.

### a. Pressure Measurement

Because of the low pressures encountered in a vacuum type tunnel, pressures must be measured with considerable precision.

Four manometer banks of 25 tubes each are used for pressure measurement. The tubes are of 3/32" I.D., 60" in length. At Mach numbers of 3 and above, it is anticipated that a manometer fluid of low density may be used; operation being that of differential manometry. At Mach 1.90 mercury has been used. Because of the comparatively short length of run a technique has been devised to decrease the damping time of the mercury column as it seeks its pressure level. This consists of evacuating the system to a value commensurate with that anticipated in the test. The pressure leads between the pressure orifice and the manometer are then clamped off as close to the model as possible. The leads are left clamped until such time after the beginning of the run that the leads from the model to the clamp have been evacuated to their run value. The clamp is then opened and the orifice pressure is indicated on the manometer board. Using this method an engineer observes the manometer board until oscillations are no longer visually discernable. A photograph of the manometer board is then taken. Data are taken from this photograph.

b. Mach Number Determination

The Mach number can be determined in several manners. Perhaps the simplest is the measurement of the angles of shock waves caused by either cones or wedges. The accuracy of this method, however, is limited by several factors: the accuracy of the fabrication of the model, the accuracy of its alignment in the flow, the distortion of the Schlieren photographs caused by density gradients in the flow, the accuracy with which shock angles can be measured, the averaging effect due to the necessity of making these measurements in a non-uniform flow, and the validity of theoretical boundary layer corrections. In view of these factors the results obtained from shock angle measurement are used only to support the results determined by other methods.

The more conventional method of determining Mach number from pressure measurements has been used. The determination of the stagnation pressure behind a normal shock wave is easily accomplished through the use of a blunt probe generating a detached wave. This pressure, relatively unaffected by small local flow inclinations, appears to be subject only to the inaccuracies of the measurement of the pressure found in the probe. Accurate determination of static pressure, however, is somewhat more difficult. (Reference 3, 4 and 5) The use of a cone or wedge, in which the pressure behind an oblique shock is measured, is subject to the same inaccuracies of machining, alignment, and local pressure variations as for its use in creating measurable shock angles. The accuracy of the use of a static probe needle is subject to several limitations. The orifice must be located sufficiently aft of the upstream end of the cylindrical portion of the needle for static pressure to approach, within negligible discrepancy, the ambient pressure; yet must be sufficiently forward that the boundary layer will have negligible influence. Local flow inclinations and the intersection of weak shock waves influence the measured pressure. Once obtained, however, the stagnation pressure aft of a normal shock (hereafter referred to as total head pressure, $P_o'$) and the freestream static pressure can be combined to obtain the stagnation pressure through the elimination of Mach number by the combining of the equations:

$$\frac{P_s}{P_o} = \left[ 1 + \left(\frac{\gamma - 1}{2}\right) M^2 \right]^{\frac{\gamma}{1-\gamma}} \qquad (1)$$

and

$$\frac{P_o'}{P_o} = \left[ \left(\frac{2\gamma}{\gamma+1}\right) M^2 - \left(\frac{\gamma-1}{\gamma+1}\right) \right]^{\frac{1}{1-\gamma}} \left[ \frac{\left(\frac{\gamma+1}{2}\right) M^2}{1 + \left(\frac{\gamma-1}{2}\right) M^2} \right]^{\frac{\gamma}{\gamma-1}} \qquad (2)$$

In the calibration of the tunnel it is difficult to justify the assumption of isentropic flow from the atmosphere to the test section. Stagnation pressure is subject to increases due to the weight of the flexible air storage bag, and the influence of heat transfer from the channel walls into the flow; and to losses through the turbulence screens, through oblique shocks, and through a condensation shock if the dew point is above a certain value.

Determination of the total loss in stagnation pressure between the atmosphere and the test section is quite a different problem than the exact determination of the component losses described above. For each Mach number configuration the total loss must be evaluated.

It has been experimentally demonstrated that the stagnation pressure is essentially a constant within the testing region of the tunnel. This appears to be plausible, for a change in $P_o$, (evidence of nonisentropic flow) would result from shock waves and heat transfer within the test section. An analysis of loss through shocks sufficient to cause the known flow nonuniformities reveals that $P_o$ does not change within the measuring accuracy. Heat transfer effect normally is limited to the thermal boundary layer. The possibility of heat release from re-evaporation of water particles is present (Ref. 6). This effect, though not rigorously understood, is at present felt to be negligible.

If sufficient static and total head pressure data are taken to yield statistically a value of $P_o$ at one point, this value can be used with $P_o'$ to obtain the Mach number and static pressure gradients within the testing area. Because of the relative absolute magnitudes of $P_s$ and $P_o'$ it is seen (see Appendix A) that if the stagnation pressure is known, then the absolute error in the computation of static pressure is considerably less than the absolute error in the total-head pressure used in the computations. In this manner it is possible, therefore, to reduce the random scatter in the static pressure due to measuring technique.

A variety of pressure probes have been designed and fabricated for calibration use. In general, however, they all utilize stainless steel hypodermic needle tubing of .065" outside diameter with .028" bore. Total head probes are blunt, static probes have conical tips of between $10^{\circ}$ and $15^{\circ}$ total vertex angle, with .024" diameter orifices between 12 and 18 body diameters aft of the conical nose section. Data from probes having one orifice have been compared with that from probes having two orifices diametrically opposed. It has not been possible to detect a significant difference between the two. Typical probes are shown in Figures 1-4, 1-5.

c. Experimental accuracies

Errors in the data are encountered in several fashions. The following discussion and analysis of error is taken from data observed while testing at a nominal Mach number of 1.90.

There is an error due to the presence of the orifice itself insofar as it disturbs the flow. Model orifice sizes have been selected in an effort to use the optimum orifice size which will have insignificant effect upon the flow, and still permit measuring equilibrium.

Errors due to leaks between the model and the measuring device can be detected and eliminated.

From a statistical analysis of pressure data, it has been found that the standard deviation of a static pressure measurement, $\sigma P_s$, is approximately .03 inches of mercury. The equation for standard deviation in pressure coefficient for small pressure changes:

$$\sigma C_p = \frac{1}{D} \sqrt{\left(\frac{\sigma P_s}{P_o}\right)^2 + \left(\frac{\sigma P_a}{P_o}\right)^2 + C_p^2 \, (\sigma D)^2} \qquad (3)$$

where $$D = \frac{\gamma}{2} M^2 \left(1 + \frac{\gamma - 1}{2} M^2\right)^{\frac{\gamma}{1-\gamma}}$$

(For derivation see Appendix B)

yields a deviation of approximately 5 per cent for a $20^{\circ}$ cone and 3 per cent for a $40^{\circ}$ cone for the static pressure deviation of .03 inches of mercury.

It has also been determined that the standard deviation in the reading of a manometer board photograph is .01 inches of mercury, which indicates that the standard deviation of a static pressure measurement, due to errors other than that incurred in reading the manometer photograph, is .026 inches of mercury.

Because of the non-uniformity of the supersonic wind tunnel stream, the measured pressure distribution over a model located in it will differ from that which would exist if the body were located in a uniform stream. In order to have the beginning of a basis for correlation between supersonic wind tunnel results and (a) theoretical calculations for the body in a uniform stream, (b) free flight data and (c) tests made in different wind tunnels, it is necessary to correct the pressure distribution measured in the non-uniform stream to that which would exist in a uniform stream.

A theoretical prediction of the first order effects of the non-uniformity of the test stream on the pressure distribution over a model was developed in Reference 7, along with a method for correcting for these effects. The effects lead to two corrections, namely the "buoyancy" and a "flow inclination" correction. A preliminary evaluation of the correction method at M = 1.90 is presented in Appendix C.

It has also been determined that the standard deviation in the reading of a manometer board photograph is .01 inches of mercury, which indicates that the standard deviation of a static pressure measurement, due to errors other than that incurred in reading the manometer photograph, is .026 inches of mercury.

Because of the non-uniformity of the supersonic wind tunnel stream, the measured pressure distribution over a model located in it will differ from that which would exist if the body were located in a uniform stream. In order to have the beginning of a basis for correlation between supersonic wind tunnel results and (a) theoretical calculations for the body in a uniform stream, (b) free flight data and (c) tests made in different wind tunnels, it is necessary to correct the pressure distribution measured in the non-uniform stream to that which would exist in a uniform stream.

A theoretical prediction of the first order effects of the non-uniformity of the test stream on the pressure distribution over a model was developed in Reference 7, along with a method for correcting for these effects. The effects lead to two corrections, namely the "buoyancy" and a "flow inclination" correction. A preliminary evaluation of the correction method at M = 1.90 is presented in Appendix C.

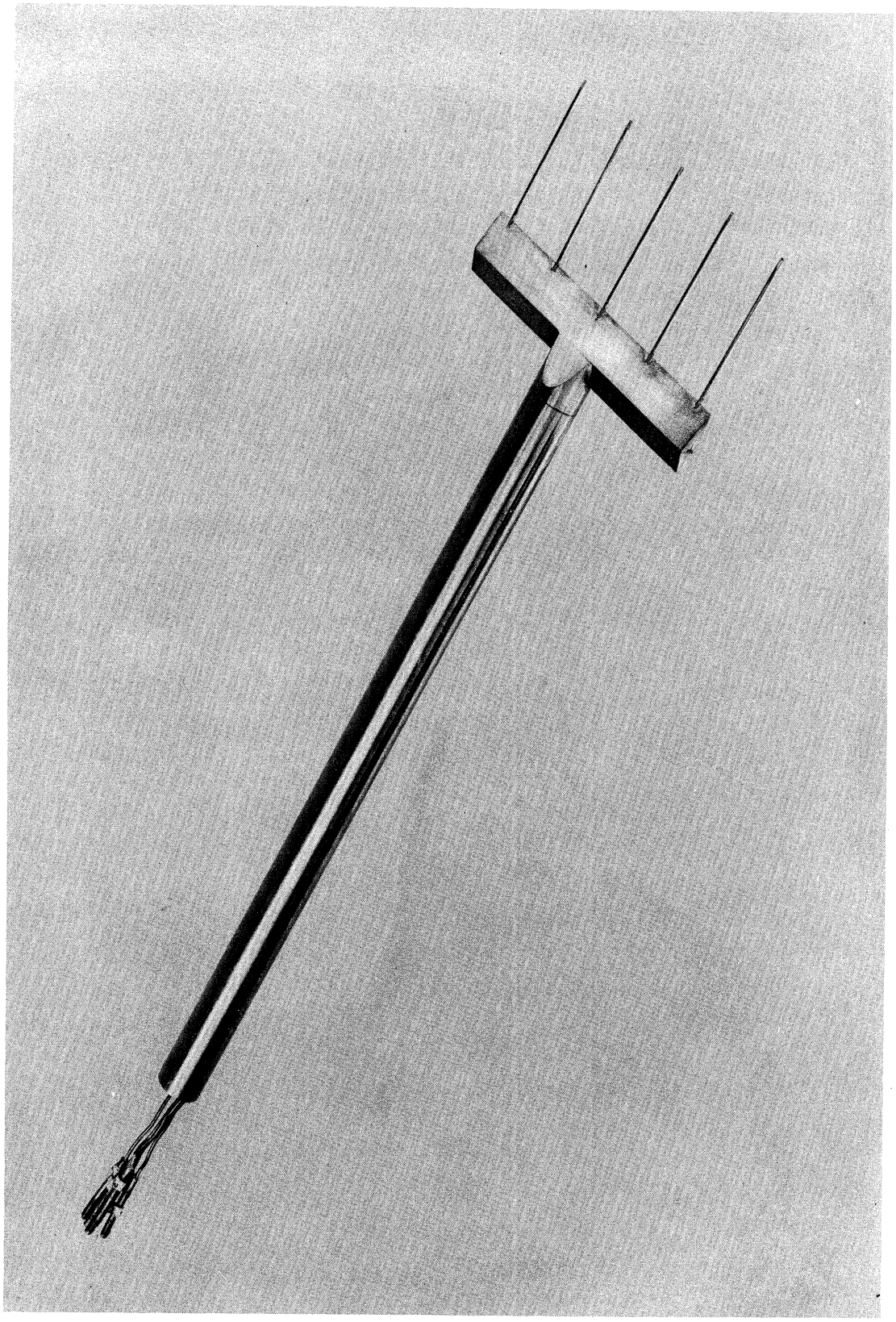

FIG. I-5 FIVE-PRONG TOTAL HEAD PROBE

## 2. MODEL SIZE CRITERIA

Limitations placed upon the size of model capable of being tested in the tunnel are made both by the critical cross-section which will pass the flow without blocking and by the length of model which can be tested without the reflection of the nose shock intersecting the subsonic wake aft of the model. Both limitations are functions of the Mach number, test, and model shape. The length of the model, when considering the scale models of conventional missile shapes, is probably the more critical dimension; that allowable being dependent upon the angle at which the nose shock is propagated. This criteria can, to a considerable extent, be determined analytically. Permissible cross-section is not, however, so easily determined, because of some of the phenomena associated with shock wave intersection and blocking itself. Experimental blocking studies are therefore made at the various Mach numbers, utilizing models of cone-cylinder configuration. These models are 6" long and of varying diameter up to 3" with total cone angles of $20^{\circ}$, $30^{\circ}$, and $40^{\circ}$. Effects of support strut thickness and vertex angle have also been studied. Results of these studies are presented in tabular form for each specific Mach number configuration.

In addition to these basic criteria it is anticipated that in the event of the testing of a model which might become critical in blocking, a simple blocking model be constructed and tested for blocking before actual testing begins.

## 3. FLOW INCLINATION

The flow inclination is determined utilizing the probe shown in Figure I-6. It is a double wedge of 3.688" span and aspect ratio of 4.1. The total leading wedge angle is $36^{\circ}$, with four pairs of orifices 0.020" in diameter spaced 1" apart. These are 0.2885" aft of the model vertex. It is possible to measure the angular position of the probe with respect to the tunnel floor to within $\pm.01^{\circ}$.

The probe is calibrated experimentally by finding the pressure differential of the two wedge faces as a function of this geometric angle. To the extent that change in local free stream flow inclinations between upper and lower corresponding orifices do not prevent the measurement of equal pressures on the wedge faces when alligned symmetrically with the flow, the local flow inclination can be determined. The geometric angle of the wedge at the interpolated zero differential is the angle of flow inclination. Within the angular range of the probe, $\pm 3^{\circ}$, the pressure differential has been found to be an essentially linear function of the angle of flow inclination. To determine the flow inclination at additional points in the flow it is necessary only to determine the geometric orientation of the wedge, measure the pressure differential of the two faces, plot the calibration curve through this point, and extrapolate the angle of zero differential. In the presence of a significant Mach number gradient it is necessary to obtain this calibration curve as a function of the local Mach number.

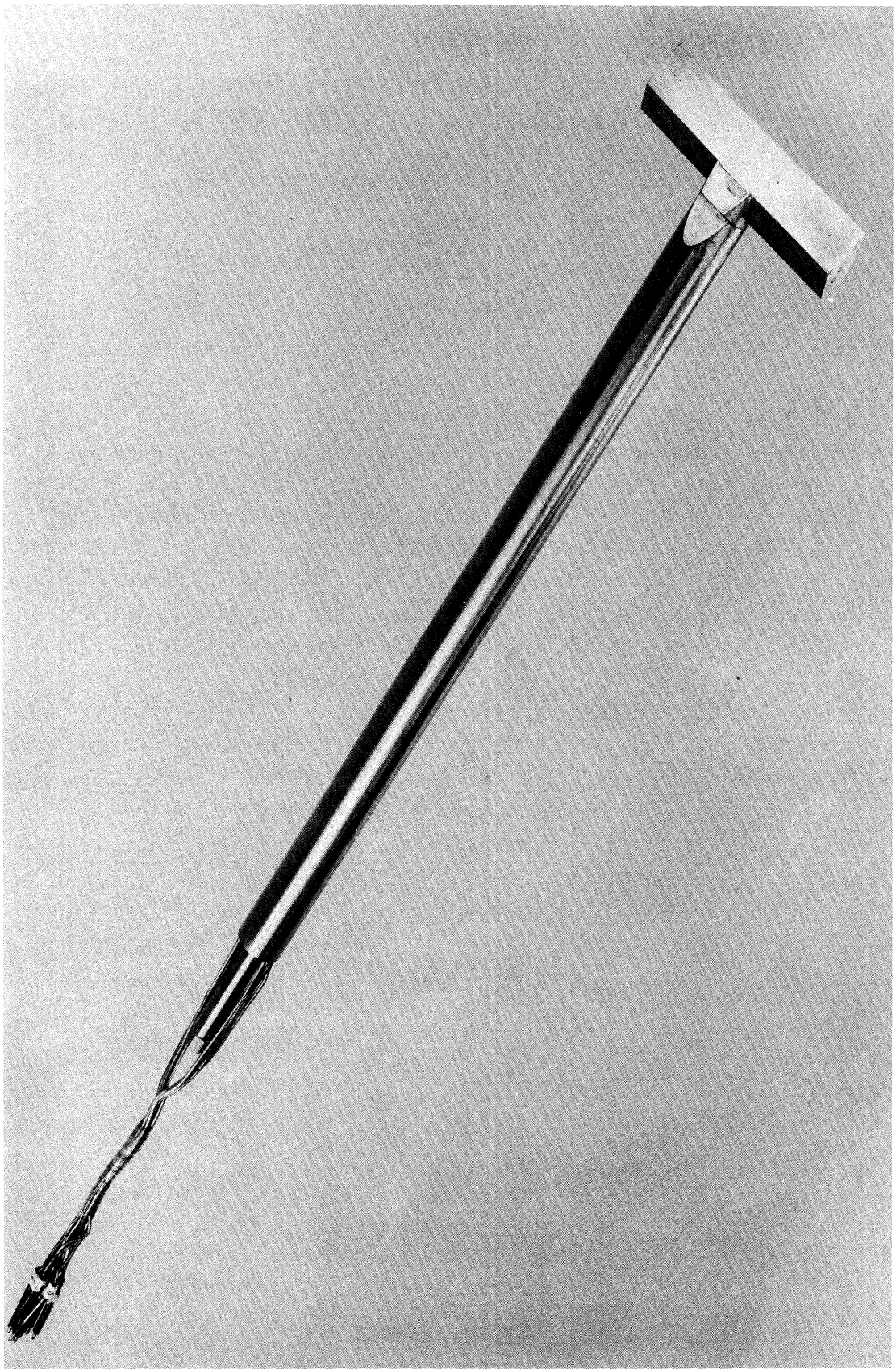

FIG. I-6 FLOW INCLINATION PROBE

## 4. LENGTH OF RUN

The length of run is considered to be the interval between the time that the normal shock passes downstream through the test section at the beginning of the run until the shock returns upstream through the test section at the end of the run. The theoretical values for length of run have been calculated from the equation as given in Reference 8.

$$t = \left(\frac{v}{\gamma a_o A_1 M_1}\right)\left(1 + \frac{\gamma-1}{2} M_1^2\right)^{\frac{\gamma+1}{2(\gamma-1)}}\left(\frac{P_f}{P_o} - \frac{P^o}{P_o}\right) \qquad (4)$$

where t = length of run
and v = vacuum tank volume
subscript o refers to test section stagnation conditions
" 1 " " the state in the test section
" f " " the state in the vacuum tank at the end of the run
superscript o refers to initial conditions in the vacuum tank

The factor $P_f/P_o$ is a function of the diffusion characteristics of the tunnel at a specific Mach number. It is affected by the configuration under test as well as the physical characteristics of the tunnel itself. This factor is determined experimentally by measuring the length of run for various vacuum pressures for a typical model and extrapolating the resulting curve to zero run time. This value, assumed to be constant, is then used in the equation yielding length of run as a linear function of $P^o/P_o$.

## 5. INFLUENCE OF DEW POINT

Much has been written from an experimental as well as a theoretical point of view concerning the effects of condensation of water on flow conditions in a supersonic wind tunnel. In general, humidity influences the flow in three ways: (a) there is a static pressure loss, and Mach number decrease, experienced through condensation shocks; (b) local deviations, caused by weak shocks known to exist in the flow, are displaced due to (a); and (c), there is the possibility of influence of re-evaporation of condensed moisture in the test section. This means that to attempt a theoretical correction for dew point influence would not only involve a linear correction in pressure but would also involve a longitudinal shift in the pressure pattern.

It is possible, however, through experimental and theoretical evidence (Ref. 9), to determine a maximum dew point which is commensurate with measuring accuracies and with economical operation at a specific Mach number.

# PART II

## AERODYNAMIC CALIBRATION AT

## NOMINAL MACH NUMBER OF 1.90

## SUMMARY

The nozzle blocks in use at the time of this calibration were designed in accordance with the analytical method derived by Kuno Foelsch (Fig. II-1, Ref. 10). A measured Mach number of 1.90 is obtained at the longitudinal centerline of the test section. Testing conditions are for a Reynold's number of approximately 4 x $10^6$ per foot.

Maximum length of run for Mach 1.90 configuration was found to be approximately 20 seconds. This length of run requires approximately 17 minutes pumping time.

A cone-cylinder 3" in diameter of 40° vertex angle will block the tunnel, while a model 3" in diameter of 30° vertex angle, and one of 2-3/4" in diameter of 40° vertex angle will pass the flow up to 12° angle of attack.

There is a gradient in static pressure to atmospheric pressure ratio in the test section of approximately .00065 per inch, with a local deviation from linear gradient due to compression and expansion regions of ±.002. This yields a Mach number gradient in the test section of approximately .0033 per inch, with a local deviation from gradient of ±.01.

The ratio of stagnation pressure in the test section to atmospheric pressure is .990 at a stagnation dew point of -25°F. This is indicative of a loss in stagnation pressure of approximately 0.29 inches of mercury.

The visible shocks appearing in the model-free flow are not the sole cause of deviations from the linear tunnel gradient; for, in probing through specific shocks it is impossible, within reading accuracy, to account for the entire deviations. Rather, compression and expansion waves are occurring in small finite bands, those visible having the greatest intensity.

A maximum flow inclination of ±.5° exists within the testing section.

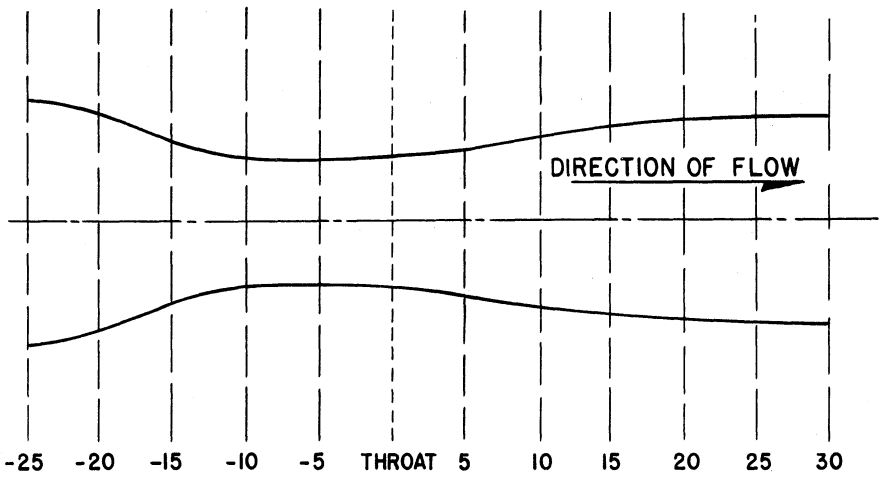


FIG. II-1 NOZZLE DIMENSIONS

X = distance along the tunnel axis in inches.
(x = 0 at the sonic throat)

Y = distance from centerline of the tunnel to the tunnel wall in inches.

| X | Y | X | Y | X | Y |
|---|---|---|---|---|---|
| -25 | 7.500 | -4 | 3.860 | 14.087 | 5.819 |
| -24 | 7.500 | -3 | 3.855 | 14.692 | 5.877 |
| -23 | 7.436 | -2 | 3.853 | 15.312 | 5.934 |
| -22 | 7.266 | -1 | 3.852 | 15.945 | 5.989 |
| -21 | 6.995 | 0 | 3.852 | 16.592 | 6.041 |
| -20 | 6.665 | 0.116 | 3.854 | 17.253 | 6.098 |
| -19 | 6.307 | 0.231 | 3.859 | 17.929 | 6.140 |
| -18 | 5.939 | 0.346 | 3.867 | 18.619 | 6.185 |
| -17 | 5.588 | 0.461 | 3.879 | 19.324 | 6.229 |
| -16 | 5.264 | 0.589 | 3.897 | 20.044 | 6.269 |
| -15 | 4.977 | 8.396 | 5.105 | 20.779 | 6.307 |
| -14 | 4.729 | 8.750 | 5.159 | 21.530 | 6.342 |
| -13 | 4.519 | 9.228 | 5.230 | 22.296 | 6.373 |
| -12 | 4.347 | 9.717 | 5.299 | 23.078 | 6.402 |
| -11 | 4.209 | 10.219 | 5.369 | 23.875 | 6.427 |
| -10 | 4.100 | 10.733 | 5.437 | 24.689 | 6.449 |
| - 9 | 4.018 | 11.260 | 5.504 | 25.519 | 6.467 |
| - 8 | 3.958 | 11.799 | 5.569 | 26.366 | 6.481 |
| - 7 | 3.915 | 12.351 | 5.634 | 27.229 | 6.491 |
| - 6 | 3.887 | 12.917 | 5.697 | 28.109 | 6.498 |
| - 5 | 3.869 | 13.495 | 5.759 | 29.000 | 6.500 |

## 1. PRESSURE AND MACH NUMBER DISTRIBUTION

An analysis of the nature of the flow in the test section was made through the use of static and total-head probes, static orifices on the sidewalls of both the test section and the nozzle, and the visual observation of weak shocks appearing in the test section. The correlation of data obtained in these fashions reveals that deviations from uniform flow can be separated into two components:

a. There exists, in the test section, a pressure gradient, resulting in a Mach number gradient, which is of the order anticipated as a result of boundary layer build up in the uniform cross section channel. This gradient in $P_s/P_b$ as seen in Figures II-2, II-3 and II-4, with the exception of certain local irregularities which shall be discussed, can be considered as a linear gradient of .00065 per inch. This yields a Mach number gradient of .0033 per inch. The influence of this gradient and results after corrections have been made for a conic type model is given in Appendix B.

b. There are certain local deviations from this linear gradient resulting from compression and expansion zones within the test section. These deviations are of the order of $\pm.002$ in $P_s/P_b$ and $\pm.01$ in Mach number.

It appears that these discrepancies from linearity result from an improper surface contour of the nozzle blocks. This conclusion is substantiated in several manners. First, it is apparent from the test section top and floor static pressure data (Fig. II-5) that the wave length of the principal expansion and compression zones is that for the reflection of weak disturbances through the 13" dimension from top to bottom. Flow inclination data reveal that the flow is inclined with respect to the horizontal, but not particularly the vertical plane in the neighborhood of the major pressure discrepancies, (Fig. II-8 and II-9). Observing the static pressure data, it is seen that the pressure is nearly uniform at similar stations across the test section, but that considerable non-uniformities exist in a vertical orientation. These, in addition to the observable shocks appearing in the model-free Schlieren photographs (Fig. II-6), tend to indicate that the major disturbances originate along the top and bottom walls. There is, however, one shock wave originating from the sidewalls which becomes visible when it is reflected from models during test. This shock crosses the centerline

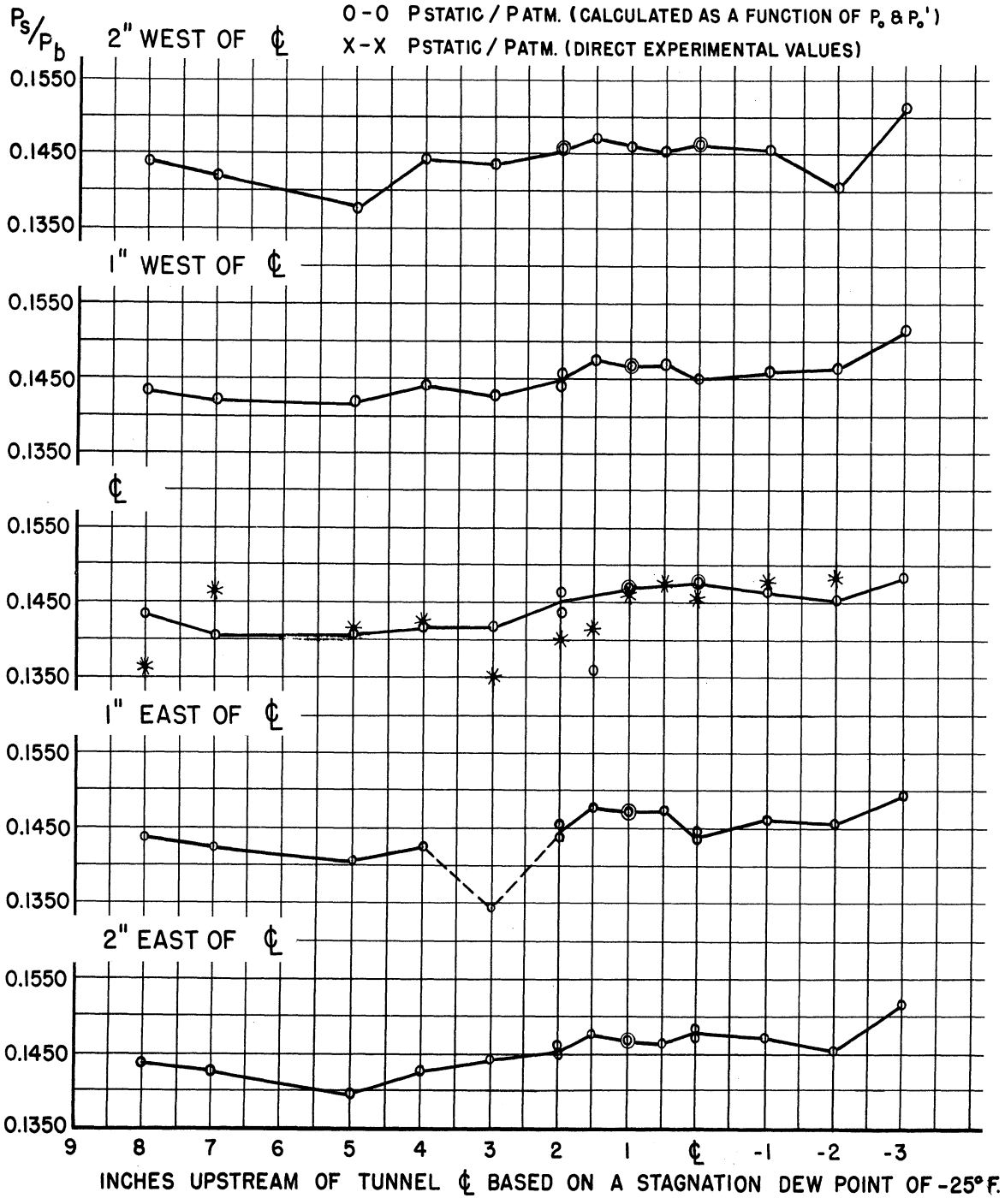


FIG. II-2 PRESSURE GRADIENT IN TEST SECTION

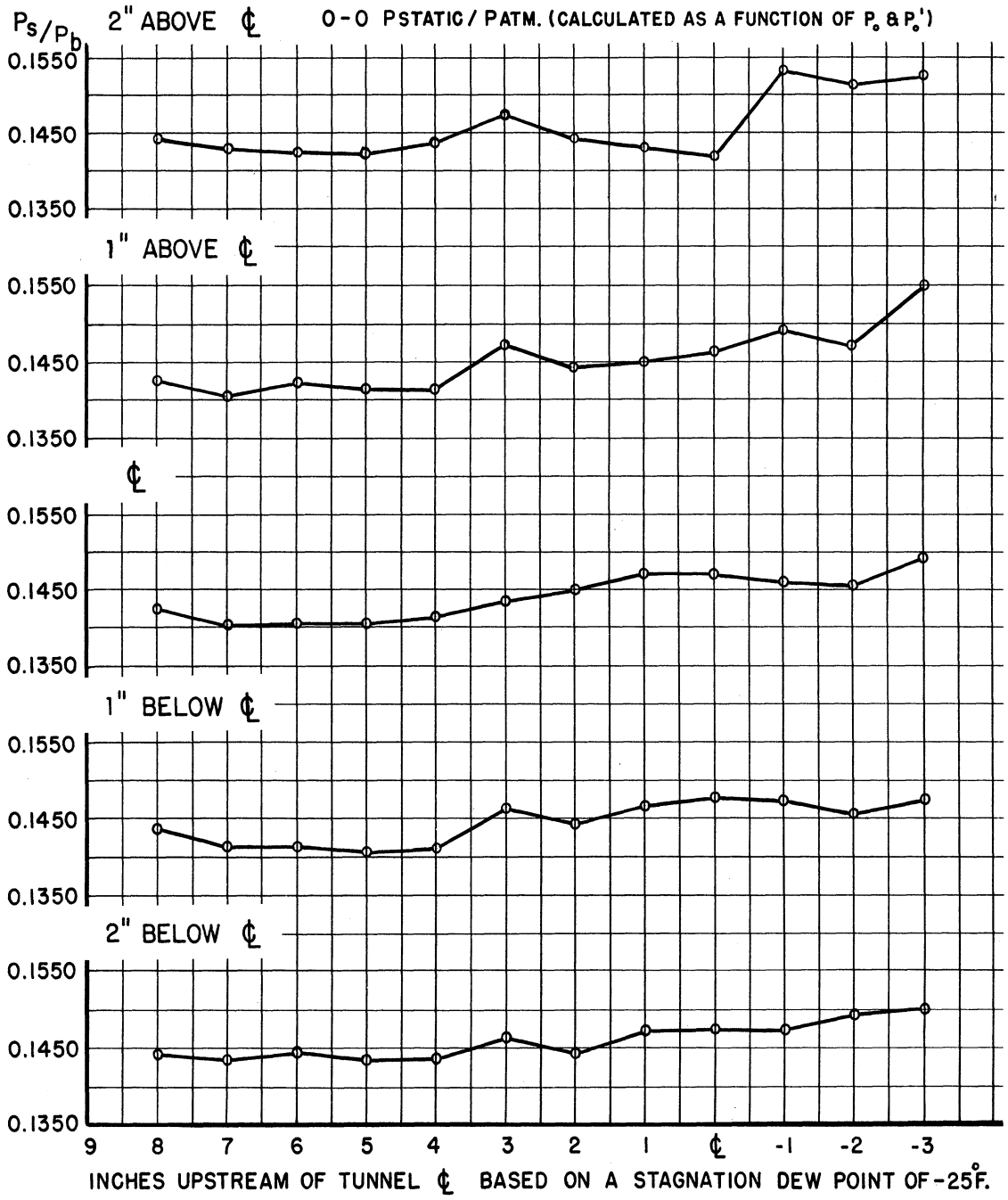


FIG. II-3 PRESSURE GRADIENT IN TEST SECTION

UNIVERSITY OF MICHIGAN SUPERSONIC WIND TUNNEL CALIBRATION-MACH=1.90

FIG. II-4 M, $P_S/P_{ATM.}$, $q/P_{ATM}$ VARIATION ALONG ℄ OF WIND TUNNEL CORRECTED TO STAGNATION DEW POINT OF -25°F.

● - PROBE VERTICAL

⊡ - PROBE HORIZONTAL

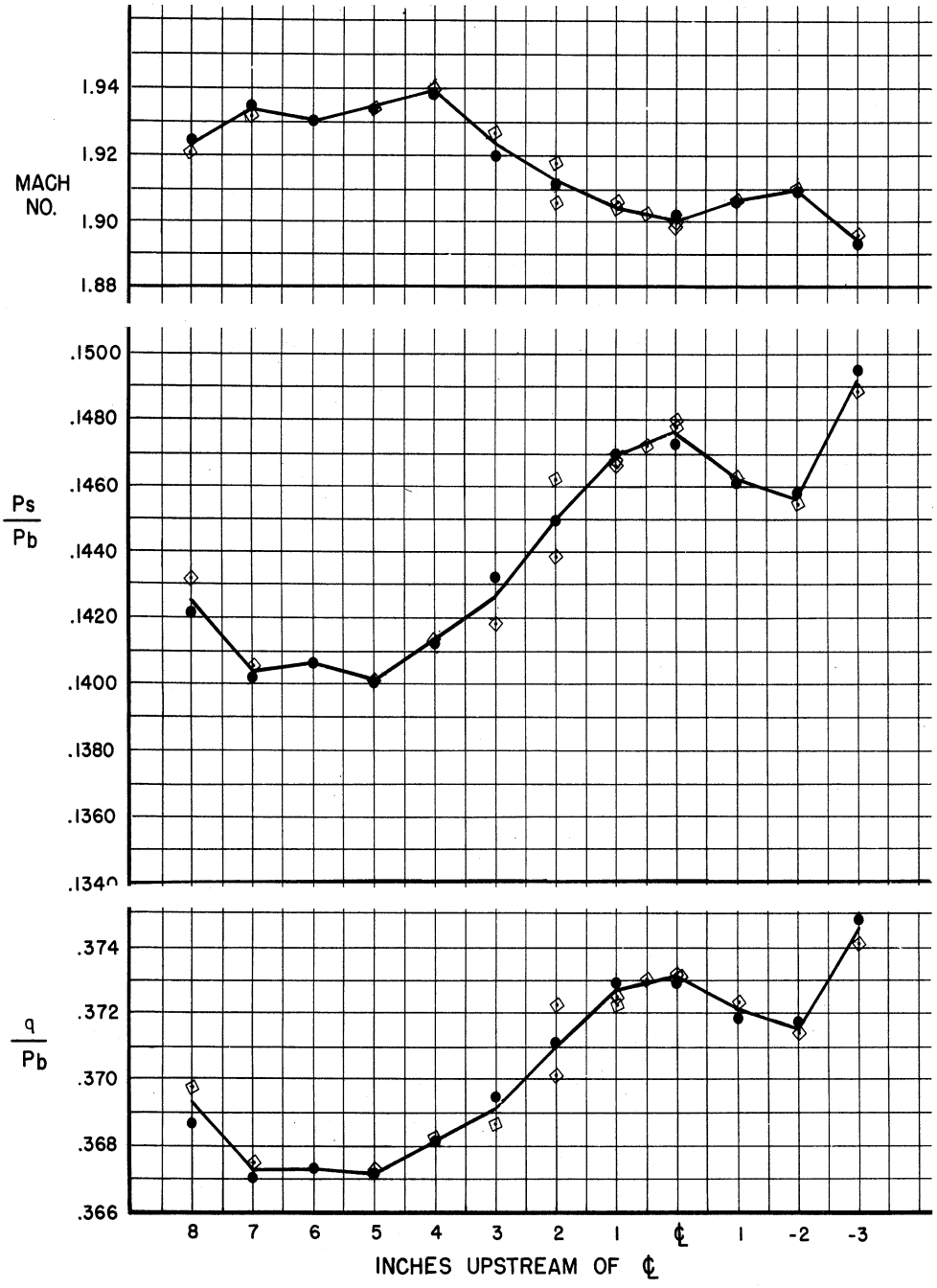

UMM-36

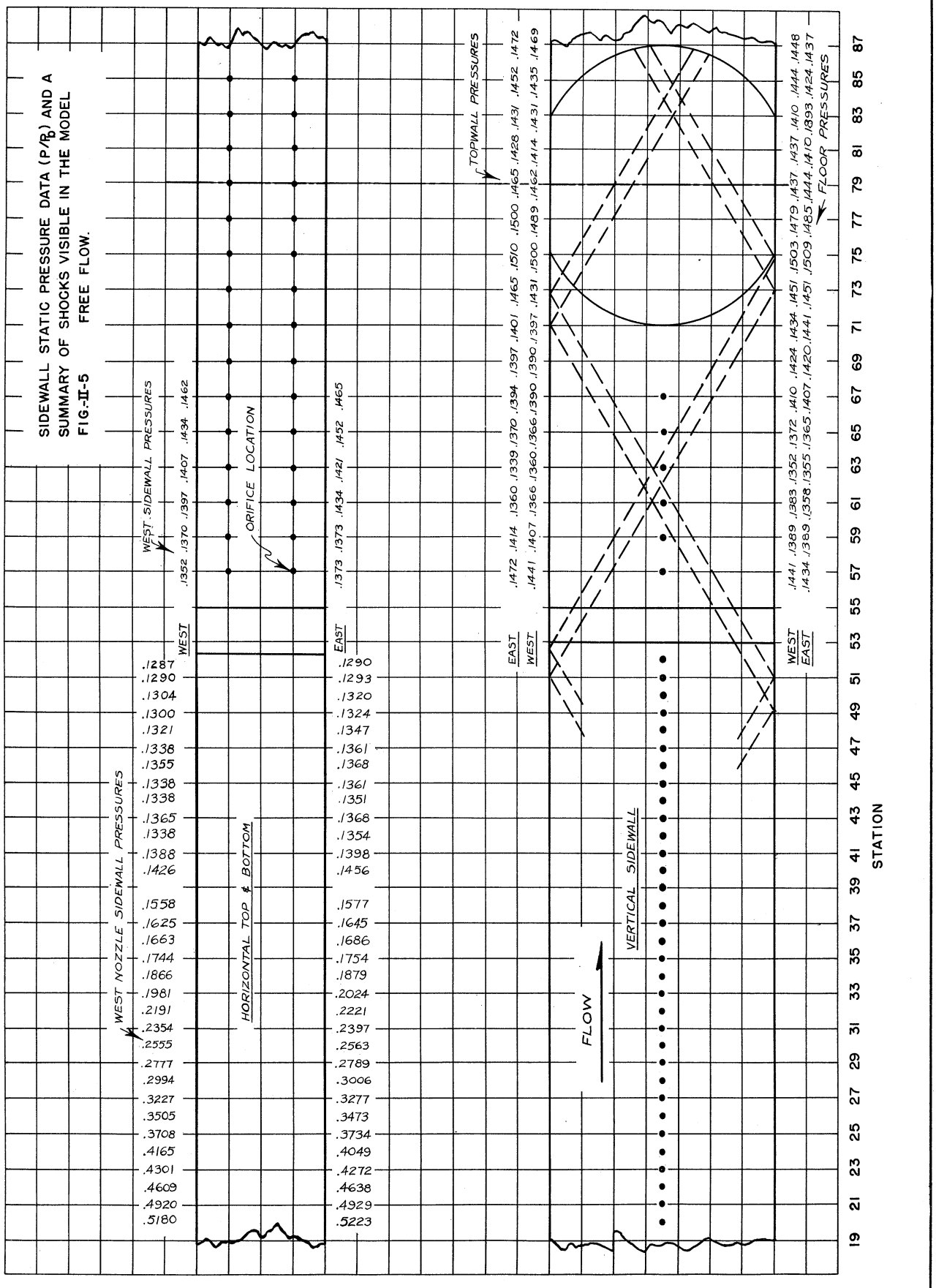
SIDEWALL STATIC PRESSURE DATA (P/P0) AND A SUMMARY OF SHOCKS VISIBLE IN THE MODEL
FIG.-II-5 FREE FLOW.
WEST SIDEWALL PRESSURES
.352 .370 .397 .407 .434 .462
WEST
.1287 .1290 .1304 .1300 .1321 .1338 .1355 .1338 .1338 .1365 .1338 .1388 .1426
WEST NOZZLE SIDEWALL PRESSURES
.1558 .1625 .1663 .1744 .1866 .1981 .2191 .2354 .2555 .2777 .2994 .3227 .3505 .3708 .4165 .4301 .4609 .4920 .5180
ORIFICE LOCATION
HORIZONTAL TOP & BOTTOM
.373 .373 .434 .421 .452 .465
EAST
.1290 .1293 .1320 .1324 .1347 .1361 .1368 .1361 .1351 .1368 .1354 .1398 .1456
.1577 .1645 .1686 .1754 .1879 .2024 .2221 .2397 .2563 .2789 .3006 .3277 .3473 .3734 .4049 .4272 .4638 .4929 .5223
TOPWALL PRESSURES
.472 .414 .360 .339 .370 .394 .397 .401 .465 .510 .500 .465 .428 .431 .452 .472
EAST
WEST
.441 .407 .366 .360 .366 .390 .390 .397 .431 .500 .489 .462 .414 .431 .435 .469
FLOOR PRESSURES
.441 .389 .383 .352 .372 .410 .424 .434 .451 .503 .479 .437 .437 .410 .444 .448
WEST
EAST
.434 .389 .358 .355 .365 .407 .420 .441 .451 .509 .485 .444 .410 .393 .424 .437
VERTICAL SIDEWALL
FLOW
19 21 23 25 27 29 31 33 35 37 39 41 43 45 47 49 51 53 55 57 59 61 63 65 67 69 71 73 75 77 79 81 83 85 87
STATION

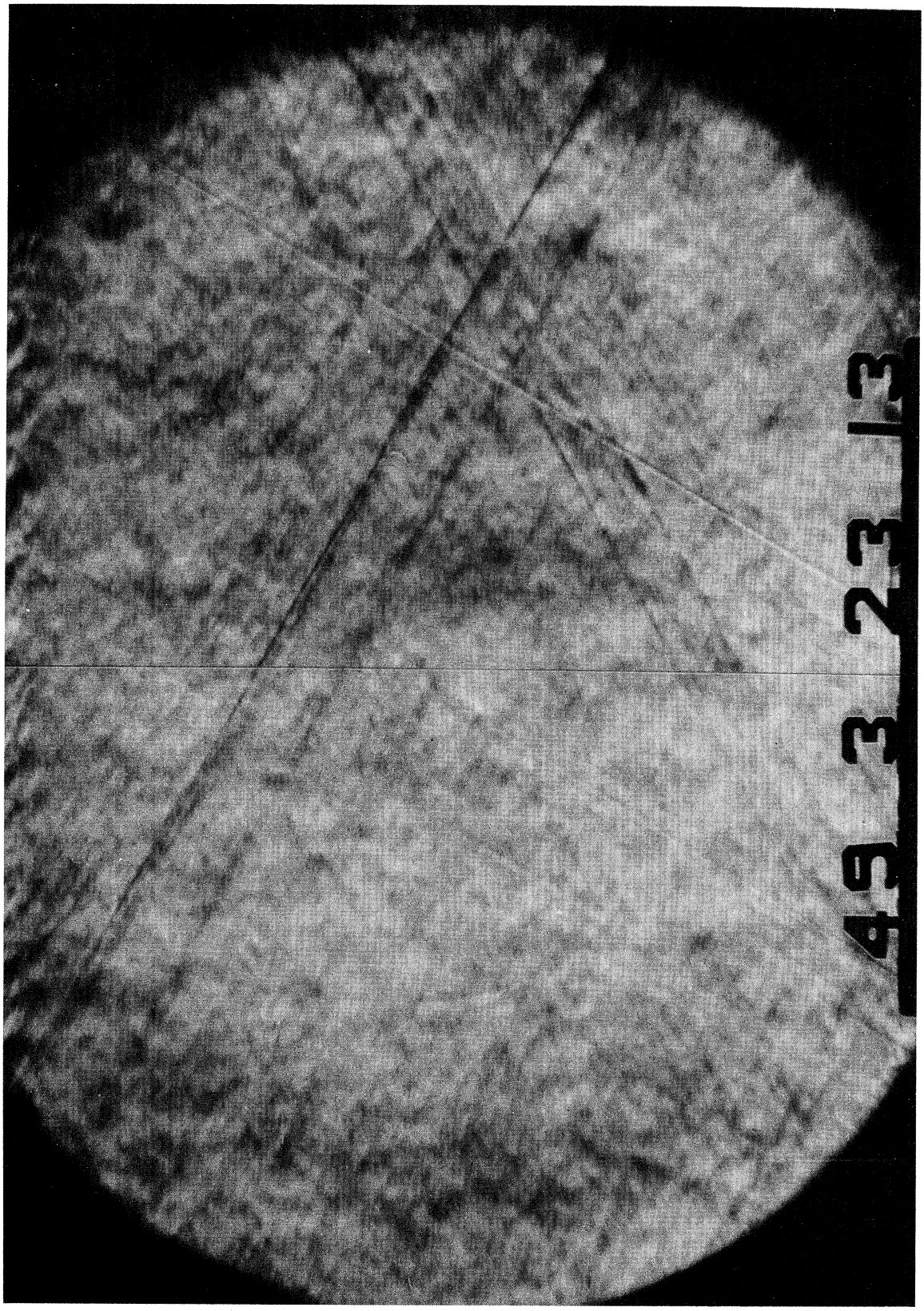


FIGURE II-6
SCHLIEREN OF MODEL-FREE FLOW AT MACH 1.90

between two and three inches forward of the window centerline, and presumably, causes the jump in pressure ratio at the 3" upstream station, as well as the scatter indicated in Figure II-4. The visible shock waves appearing in the test section have been traced upstream and found to originate in the nozzle.

The static pressure calibration curve presented in this report was calculated as a function of the total pressure immediately downstream of a normal shock wave and the stagnation pressure, in accordance with the method described previously in this report. The value of the stagnation pressure was obtained through an extensive analysis of the flow at positions 1.04" and 1.27" upstream of the longitudinal centerline at a range in dew point of the test air of from -30° to -22°F. This analysis yielded a value of the ratio of stagnation pressure to atmospheric pressure of .990. This indicates a loss of approximately 0.29" of mercury in stagnation pressure between the atmosphere and the point under consideration.

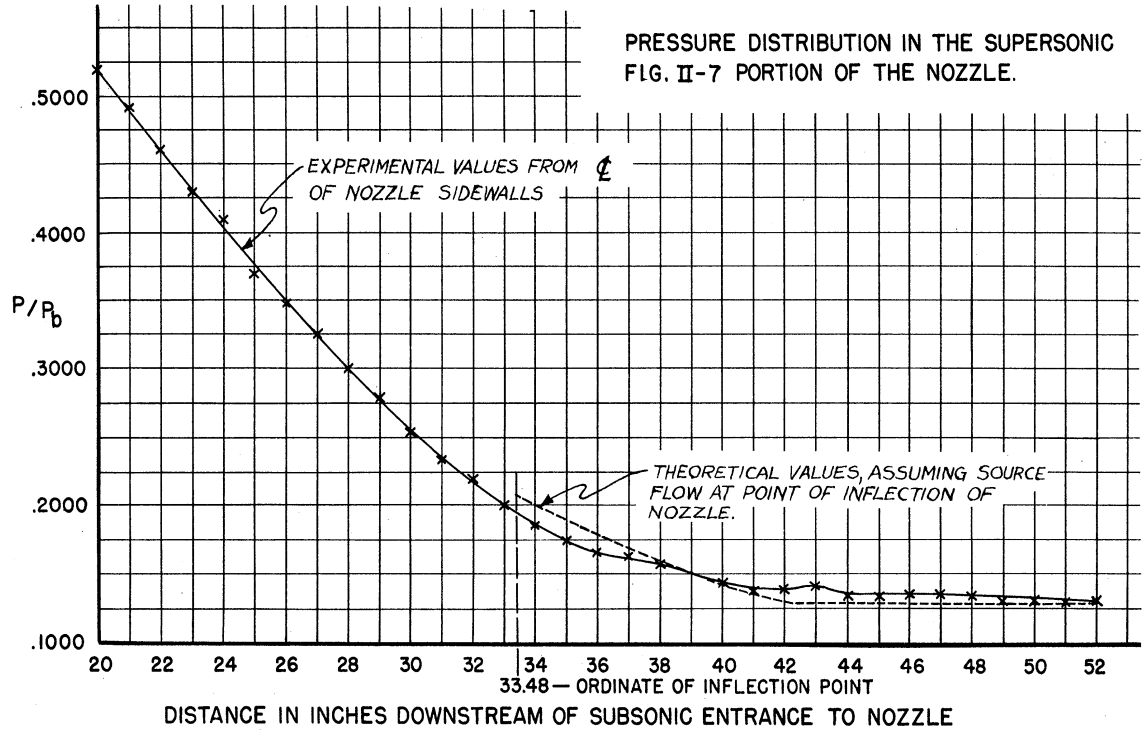

## 2. BLOCKING

In blocking tests it was found that a 2-3/4" diameter cone-cylinder of vertex angle 40° and length 6" would pass the Mach 2 flow at angles of attack up to ±12°. No greater angle of attack was tested. This model was mounted on a sting of 1/2" diameter which was mounted in the force ring strut of 1/2" thickness, 4" depth and 28° total leading angle. A 3" diameter cone-cylinder of vertex angle 30° and length of 6" likewise passed the flow, while a 3" diameter cone-cylinder vertex angle of 40° would not.

No attempt was made toward finding the maximum allowable strut thickness and leading angle; however a strut of 3/8" thickness and 20° total vertex angle, one of 1/2" thickness and 20° vertex angle, one of 1/2" thickness and 30° vertex angle, and one of 5/8" thickness and 30° vertex angle were used in an attempt to evaluate their effects upon blocking. It was not possible to determine any effect which this change in strut configuration had upon size of model which could be tested in the tunnel without blocking. In all cases, a model 3" diameter with vertex angle of 40° blocked the tunnel; while one of 3" in diameter of 30° vertex angle or one of 2-3/4" in diameter and 40° vertex angle would not block.

The starting vacuum pressure was varied from 0.877 psia to 4.72 psia and in each case flow was established around a cone- cylinder 1-1/2" in diameter of 40° vertex angle mounted on the 1/2" x 30° force ring without blocking. In a run made with initial vacuum of 6.57 psia, however, satisfactory flow was not established past the strut.

These results are shown tabulated in Figure II-8.

FIGURE II-8

| MODEL | ANGLE OF ATTACK | STRUT | FLOW CONDITIONS |
|---|---|---|---|
| 3"D x 40° | 0 | 1/2 x 30° | Blocked with stub shield |
| 3"D x 40° | 0 | 1/2 x 30° | Blocked |
| 3"D x 40° | 0 | 1/2 x 20° | Blocked |
| 1-1/2"D x 40° | 0 | 1/2 x 30° | Flow not established in 4 seconds |
| 1-1/2"D x 40° | 0 | 1/2 x 30° | Flow established in 5 seconds |
| 1-1/2"D x 40° | 0 | 1/2 x 30° | Windshield-sidewall slots closed. Flow not established in 6 seconds |
| 1-1/2"D x 40° | 0 | 1/2 x 30° | Initial $P/P_o$ = .535, flow not established |
| 1-1/2"D x 40° | 0 | 1/2 x 30° | Initial $P/P_o$ = .67, flow established |
| 3"D x 30° | 0 | 3/8 x 20° | Passed |
| 3"D x 30° | 0 | 1/2 x 20° | Passed |
| 2-3/4"D x 40° | +12 | 1/2 x 30° | Passed |
| 2-3/4"D x 40° | -12 | 1/2 x 30° | Passed |
| 2-3/4"D x 40° | 0 | 5/8 x 30° | Passed with stub shield in place |
| 2-3/4"D x 40° | 0 | 5/8 x 30° | Passed with no stub shield |

## 3. FLOW INCLINATION

The flow inclination probe and its use have been described. For the calibration at Mach number 1.90 the wedge pressure differential was measured utilizing oil of specific gravity .827 in a differential manometer.

The flow inclination in the test section was probed from 9" forward to 4" aft of the test section centerline. Maximum flow inclination with respect to the horizontal plane was found to be $\pm.5^{\circ}$, while the inclination in the region upstream of the centerline was from $-.1^{\circ}$ to $+.3^{\circ}$. With respect to the vertical plane the inclination was $\pm.3^{\circ}$, while upstream of the centerline it was from $-.3^{\circ}$ to $+.1^{\circ}$. The repeatability of these values was within $\pm.05^{\circ}$. The flow inclination patterns are shown in Figures II-9 and II-10. In these data it is interesting to observe the close correlation between the flow inclination and the shocks appearing in the model-free flow. It is noted that, of the visible shocks, the strongest is reflected from the upper surface and passes through the horizontal plane of the centerline at a point approximately 3" aft of the longitudinal centerline. In this region inclination changes from positive to negative in the manner anticipated, followed by a change to a less negative inclination, indicative of the shock appearing from the tunnel floor.

Although shock waves in the vertical plane cannot be observed directly, their intersection with models can be seen. It has been noted that a shock wave in the vertical plane strikes small models at a point between two and three inches forward of the centerline. This, too, is seen in the flow inclination data.

UNIVERSITY OF MICHIGAN SUPERSONIC WIND TUNNEL CALIBRATION - MACH = 1.90

FIG. II-9 FLOW INCLINATION

PROBE HORIZONTAL, POSITIVE INCLINATION INDICATES POSITIVE ANGLE OF ATTACK FOR MODEL AT GEOMETRIC ZERO.

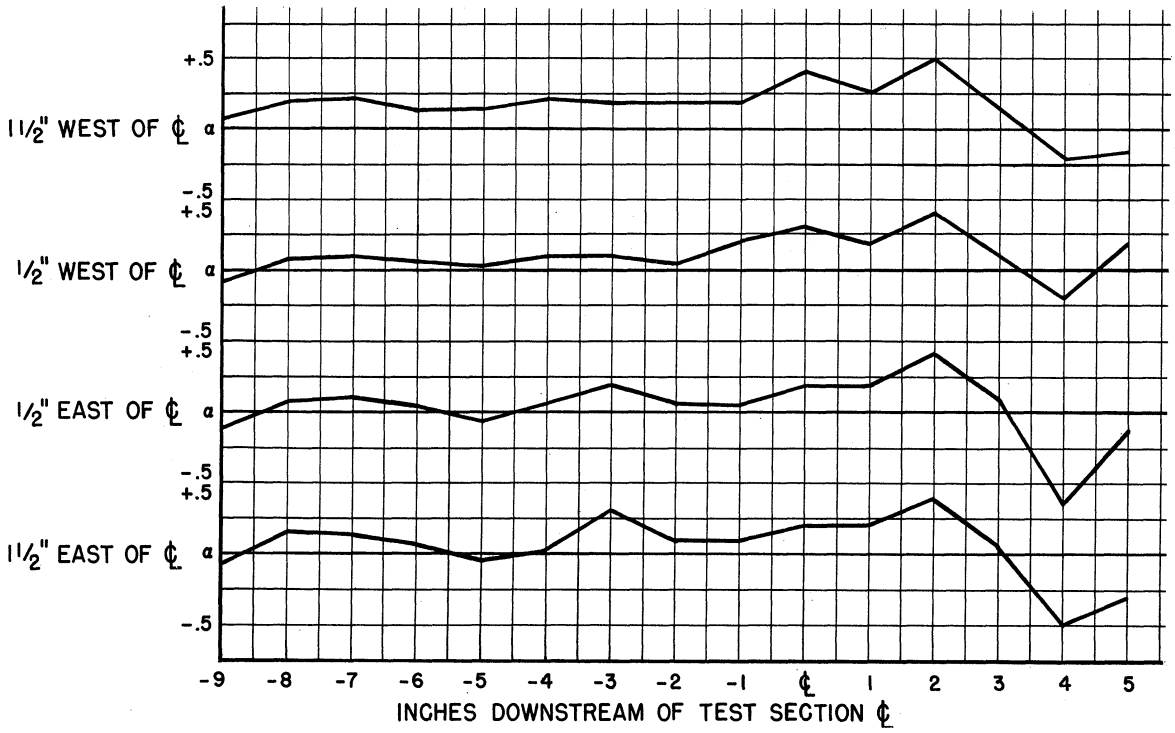


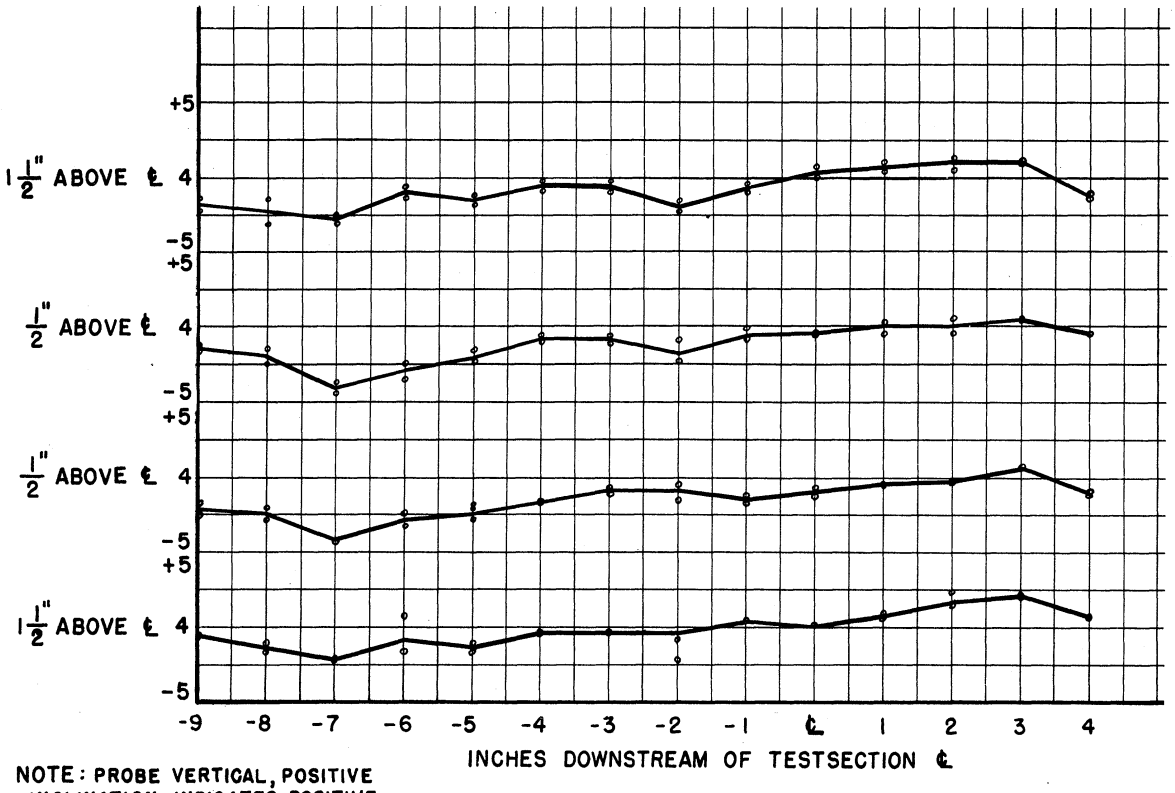


NOTE: PROBE VERTICAL, POSITIVE INCLINATION INDICATES POSITIVE ANGLE OF YAW FOR MODEL AT GEOMETRIC ZERO.

FIG. II-10 FLOW INCLINATION

## 4. LENGTH OF RUN

Experimental values of length of run as a function of initial vacuum tank pressure are shown in Figures II-11 and II-12. The discrepany between theoretical and experimental values of length of run is largely due to the fact that in deriving the empirical equation for t, the value of $P_f/P_o$ for zero length of run was used. This value is that for pressure recovery when a normal shock wave stands in the test section. In an actual run, diffusion, rather than through a normal shock wave, is through a series of oblique and normal waves dependent upon the model configuration, the diffuser geometry, and the instantaneous pressure in the vacuum tank. Pressure recovery is greater through these oblique waves than through a normal wave in the test section resulting in greater length of run than the equation would indicate.

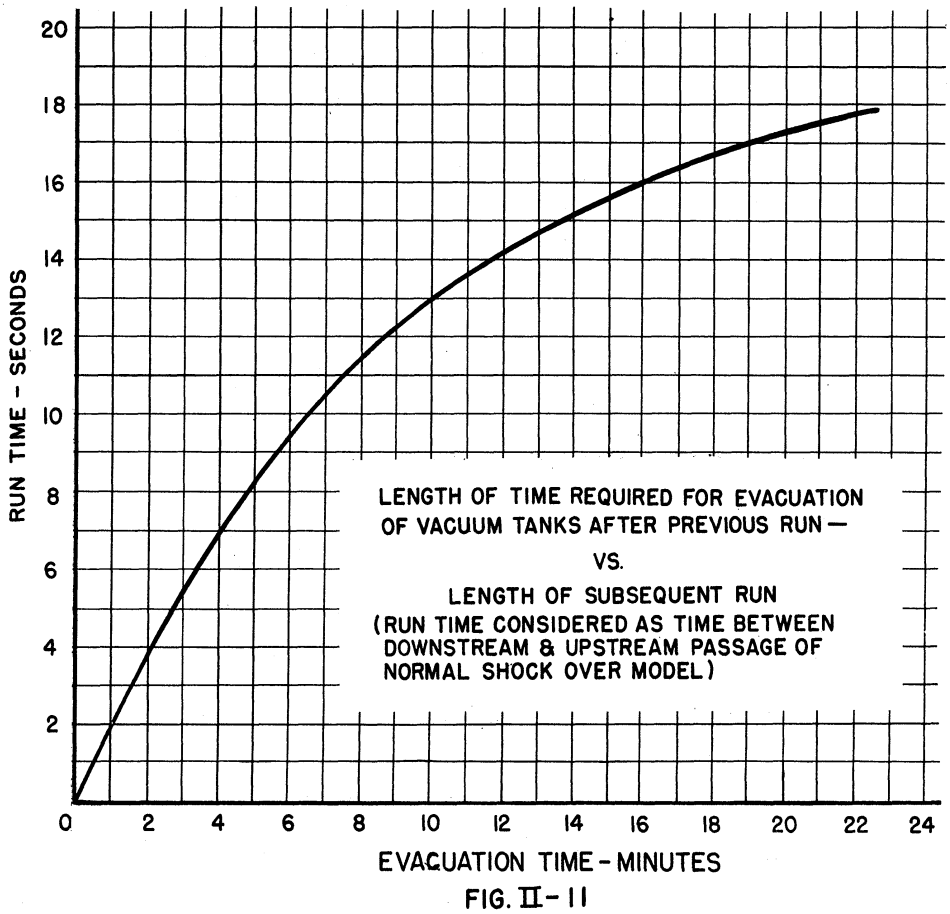


FIG. II-11

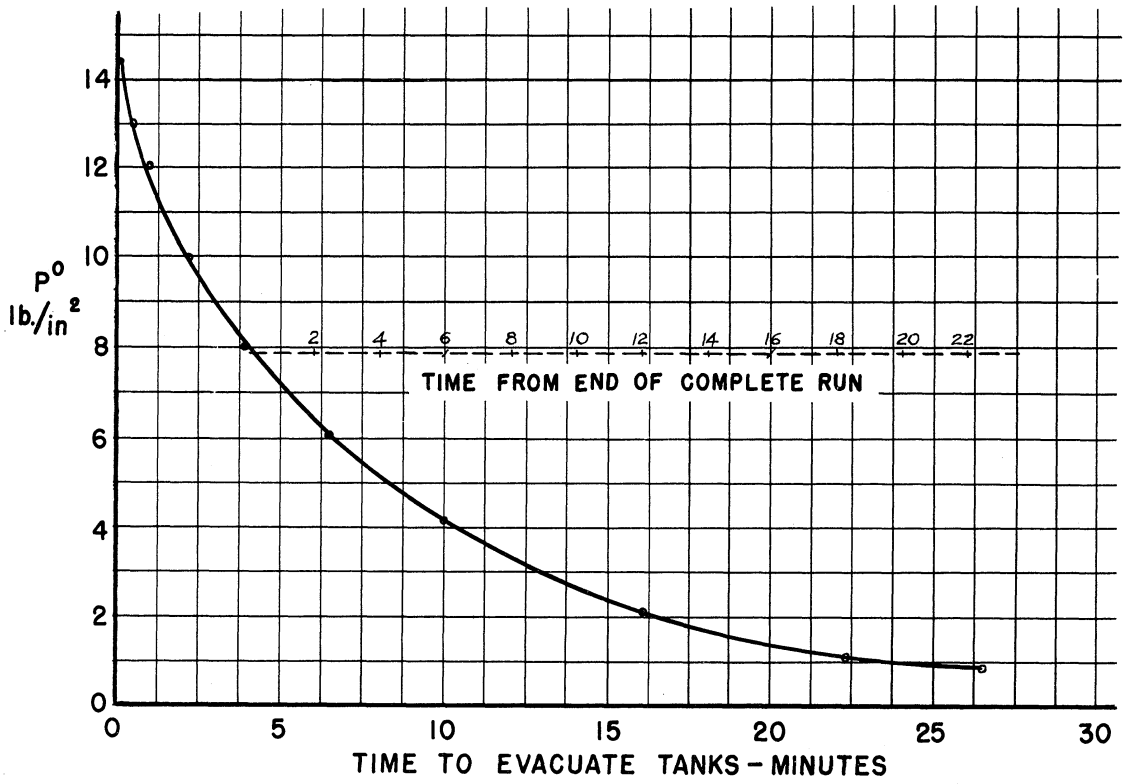


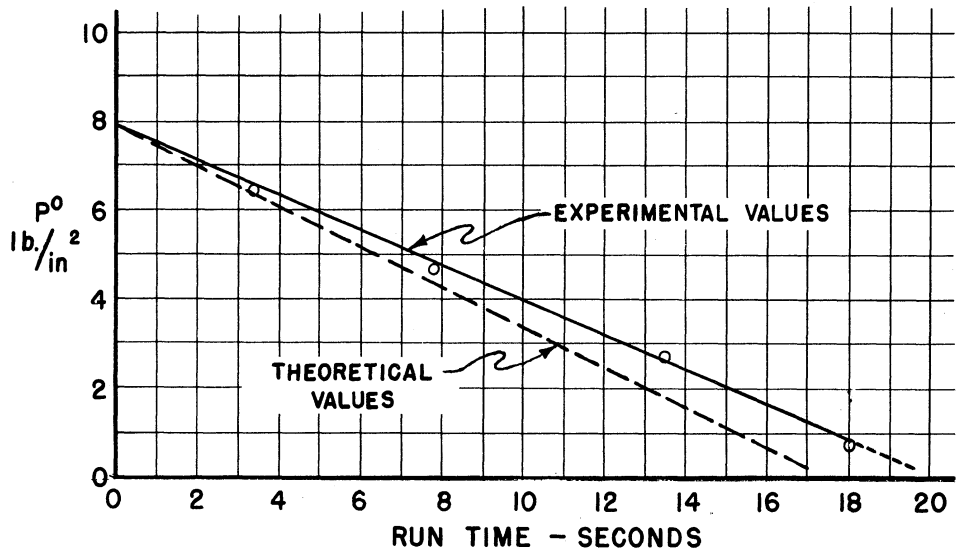


RUN TIME CONSIDERED FROM DOWNSTREAM TO UPSTREAM PASSAGE OF NORMAL SHOCK OVER MODEL.

Figure II - 12

VACUUM TANK PUMP DOWN AND RUN TIME AS A FUNCTION OF VACUUM TANK PRESSURE

## 5. INFLUENCE OF DEW POINT

In the calibration of the tunnel it is not the details of the condensation phenomena which are desired, but rather the determination of a dew point criteria for which dew point effects are negligible with respect to other errors. As previously pointed out, static pressures measured have a standard deviation of .03" mercury. This standard deviation then leads to a theoretical upper limit of -15° F for the allowable dew point of the stagnation air (Ref. 9). During the course of routine tests, this value of the upper limit of dew point has been verified as shown in Figure II-13. The data shown in this figure were taken from a sidewall orifice. The figure indicates that for dew points below -15°F, the increase in static pressure due to condensation is masked in the inaccuracy of the determination of static pressure.

FIG. II-13 VARIATION, AS A FUNCTION OF DEW POINT, OF THE RATIO STATIC PRESSURE TO ATMOSPHERIC PRESSURE TEN INCHES UPSTREAM OF TUNNEL WINDOW CENTER LINE (WALL ORIFICE 569)

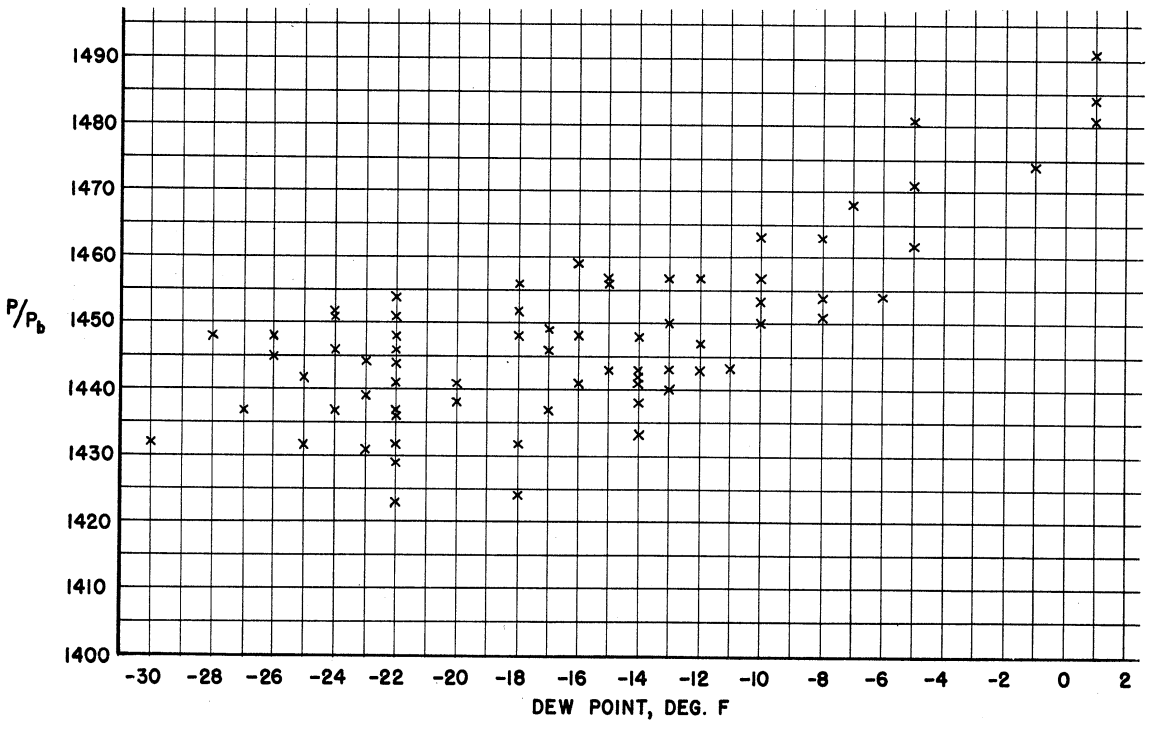

## APPENDIX A

Accuracy of the determination of static pressure from stagnation and total head pressures.

From the equations:

$$\frac{P_s}{P_o} = \left[1 + \left(\frac{\gamma - 1}{2}\right) M^2\right]^{\frac{\gamma}{1-\gamma}}$$

and

$$\frac{P_o'}{P_o} = \left[\left(\frac{2\gamma}{\gamma + 1}\right) M^2 - \left(\frac{\gamma - 1}{\gamma + 1}\right)\right]^{\frac{1}{1-\gamma}} \left[\frac{\frac{\gamma + 1}{2} M^2}{1 + \left(\frac{\gamma - 1}{2}\right) M^2}\right]^{\frac{\gamma}{\gamma - 1}}$$

the Mach number was eliminated to yield:

$$\frac{P_o'}{P_o} = \left\{\left(\frac{4\gamma}{\gamma^2 - 1}\right)\left[\left(\frac{P_s}{P_o}\right)^{\frac{1-\gamma}{\gamma}} - 1\right] - \left(\frac{\gamma - 1}{\gamma + 1}\right)\right\}^{\frac{1}{1-\gamma}}$$

$$\left\{\frac{\left(\frac{\gamma + 1}{\gamma - 1}\right)\left[\left(\frac{P_s}{P_o}\right)^{\frac{1-\gamma}{\gamma}} - 1\right]}{\left(\frac{P_s}{P_o}\right)^{\frac{1-\gamma}{\gamma}}}\right\}^{\frac{\gamma}{\gamma - 1}}$$

This was reduced to

$$\Delta P_s = \frac{1}{K}\left[\frac{\Delta P_o}{P_o}\left(KP_s - P_o'\right) + \Delta P_o'\right]$$

where K is a function of $\frac{P_s}{P_o}$ and $\gamma$

Thus it is seen that in computing $P_s$ from $P_o$ and $P_o'$; errors in $P_s$ are essentially $\frac{1}{K}$ times error in $P_o'$, providing that error in $P_o$ is very small.

The factor K has been computed for various Mach numbers. Between Mach 1.85 and 2.00, K is between 16.00 and 16.51.

## APPENDIX B

Standard deviation of pressure coefficient due to error in pressure measurement.

Using the expression for pressure coefficient as developed in any standard text on compressible fluid flow:

$$C_p = \frac{P_s - P_a}{\frac{\gamma}{2} P_s M_1^2}$$

One can introduce the parameter $P_o$ to yield:

$$C_p = \frac{P_s/P_o - P_a/P_o}{\frac{\gamma}{2} P_s/P_o \, M_1^2} = \frac{P_s/P_o - P_a/P_o}{D}$$

where $$D = \frac{\gamma}{2} M_1^2 \left( 1 + \frac{\gamma - 1}{2} M_1^2 \right)^{\frac{\gamma}{1-\gamma}}$$

Differentiating, and solving for the standard deviation $\sigma C_{p_1}$ one obtains:

$$\sigma C_p = \frac{1}{D} \sqrt{\left(\frac{P_s}{P_o}\right)^2 + \left(\frac{P_a}{P_o}\right)^2 + C_p^2 \, \sigma D^2}$$

where $$\sigma D = D \left[ \frac{2}{M} + \frac{\gamma M}{1 + \frac{\gamma - 1}{2} M^2} \right] \sigma M$$

## APPENDIX C

### Pressure Correction Evaluation.

An evaluation of the method of correcting (Ref. 7) for the effects of non-uniformities in the Mach 1.90 test section flow on the pressure distribution over a model has been made. Test results are presented here for a 15° total angle cone, eight inches in length. During the tests, the cone vertex was located 6.8" forward of the window centerline and the cone axis was aligned with the horizontal axis of the tunnel. The model contained 32 static pressure orifices arranged in four rows, two rows in the vertical plane and two rows in the horizontal plane through the cone axis. The eight orifices in each row were spaced one inch apart with the first orifice of each row 3/4" aft of the cone vertex.

The corrections applied to the data may be divided into two parts, a buoyancy correction and a correction for flow inclinations.

The buoyancy correction takes into account the variation of ambient static pressure in the wind tunnel at each orifice location. The ambient static pressure values along the longitudinal centerline as presented in the calibration report were used in the calculation of pressure coefficient.

The correction for local flow inclination was made by averaging the values of $C_p$ measured for any two diametrically opposed orifices. This correction should eliminate any effect on the value of $C_p$ due to flow inclinations in vertical and horizontal planes. Figure II-14 shows the measured $C_p$ distribution before corrections for test section flow non-uniformities were made, and Figure II-15 shows the distribution after the corrections were made.

FIG. II-14 $C_p$ DATA FOR 15° CONE BEFORE CORRECTION FOR NON-UNIFORMITY OF FLOW

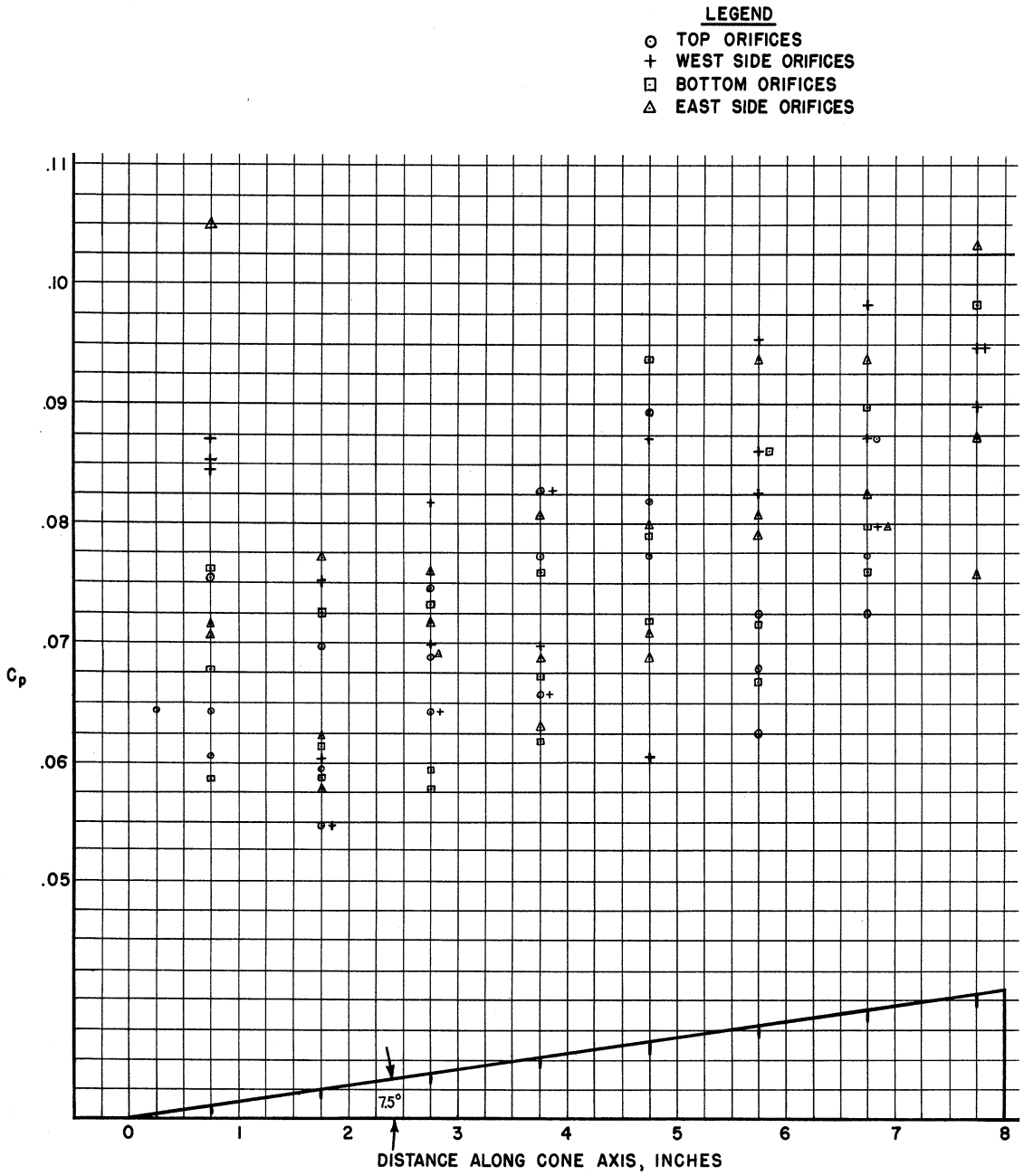

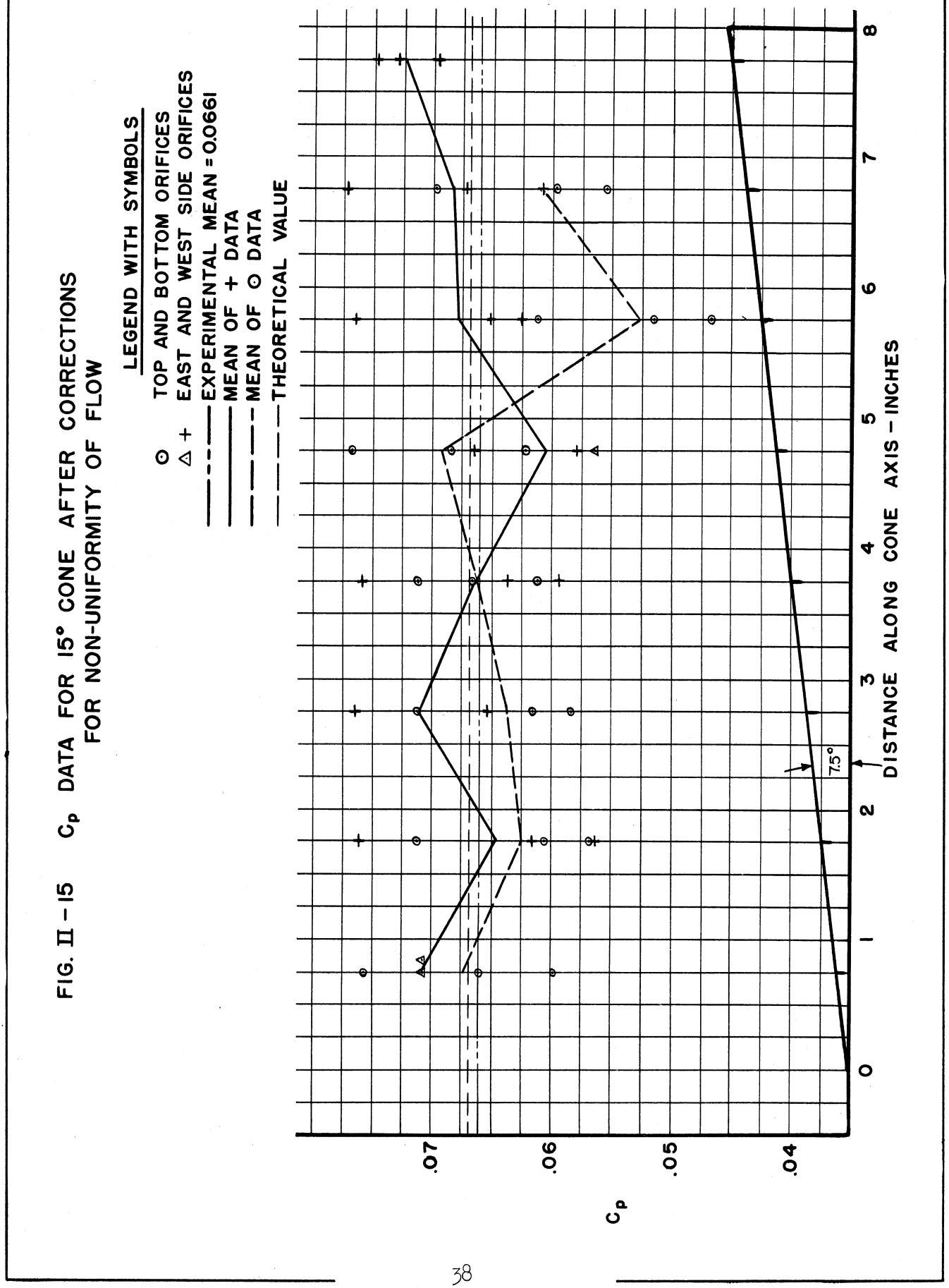


FIG. II – 15 $C_p$ DATA FOR 15° CONE AFTER CORRECTIONS FOR NON-UNIFORMITY OF FLOW

REFERENCES

1. WTM - 111 Final Report on Static Calibration of the U.M.E.R.I. Supersonic Wind Tunnel Balance System. J. L. Raymond and E. T. Clark July 27, 1947

2. WTM - 91 Development Tests on Lift-Moment Combination of Sting Type Balance System. Rossow and Bailey May 13, 1949

3. Bumblebee Aerodynamics Symposium November 4-5, 1945 "Pressure Distributions Over a Cylinder with Conical or Hemispherical Nose" L. L. Cronvich

4. NACA RM No. L8102 Investigation of Two Pitot-Static Tubes At Supersonic Speeds. Hasel and Coletti November 19, 1948.

5. Douglas Aircraft Report No. SM-133322 Pressure Distribution on a Cylinder Preceded by a Cone in a Axial Supersonic Flow. E. W. Graham July 21, 1948

6. California Institute of Technology Doctorial Thesisis on -- Investigations of Spontaneous Condensation, (1949) Richard M. Head

7. WTM - 112 Pressure Corrections for Slender Bodies of Revolution in Non-Uniform Supersonic Stream. M. V. Morkovin and J. S. Murphy July 29, 1949

8. EMP - 16 Interim Report. Intermittent Supersonic Wind Tunnel. R. I. Schneyer

9. WTM - 116 Influence of Dewpoint on the Mach Number and Pressure in the Test Section. R. C. Frost August 11, 1949

10. NA-46-235-2 A New Method of Designing Two-Dimensional Laval Nozzles for a Parallel and Uniform Jet" Kuno Koelsch 1946

## DISTRIBUTION

Distribution of this report is made in accordance with ANAF-GM Mailing List No. 9, dated September 1949, to include Part A, Part B, and Part C.